PERGAMON

Computerized Medical Imaging and Graphics 24 (2000) 349–357

Computerized Medical Imaging and Graphics

www.elsevier.com/locate/compmedimag

MRI brain image segmentation by multi-resolution edge detection and region selection

H. Tang[a,b,c,*], E.X. Wu[a], Q.Y. Ma[b], D. Gallagher[c], G.M. Perera[a], T. Zhuang[d]

[a]*Department of Radiology, Hatch NMR Research Center, Columbia University, 710 West 168th St., New York, NY 10023, USA*
[b]*Department of Electrical Engineering, Columbia University, 1312 Mudd, 500 West 120th St., New York, NY 10027, USA*
[c]*Obesity Research Center, St. Luke's Roosevelt Hospital, Columbia University, 1090 Amsterdam Ave., New York, NY 10025, USA*
[d]*Department of Biomedical Engineering, Shanghai Jiao Tong University, Shanghai 200030, People's Republic of China*

Received 7 February 2000; accepted 16 May 2000

Abstract

Combining both spatial and intensity information in image, we present an MRI brain image segmentation approach based on multi-resolution edge detection, region selection, and intensity threshold methods. The detection of white matter structure in brain is emphasized in this paper. First, a multi-resolution brain image representation and segmentation procedure based on a multi-scale image filtering method is presented. Given the nature of the structural connectivity and intensity homogeneity of brain tissues, region-based methods such as region growing and subtraction to segment the brain tissue structure from the multi-resolution images are utilized. From the segmented structure, the region-of-interest (ROI) image in the structure region is derived, and then a modified segmentation of the ROI based on an automatic threshold method using our threshold selection criterion is presented. Examples on both T1 and T2 weighted MRI brain image segmentation is presented, showing finer brain tissue structures.

Keywords: Image segmentation; Multi-resolution edge detection; Multi-scale filtering; Region-growing; Threshold selection

1. Introduction

Many methods have been proposed for MRI brain tissue segmentation [1]. Since the boundaries of different tissues in MRI brain images are indistinct and the intensities of the white and gray matter are very close, the edge-based segmentation methods may not provide satisfactory results. Thus the knowledge-based methods, e.g. clustering algorithms for brain tissue classification [2], integrated edge and region detection [3], and deformable template-based methods [4–5], are being investigated for automatic and accurate image segmentation. Knowledge-based methods [6] include several pattern recognition procedures needing a priori anatomical knowledge of the region-of-interest and the human training data set. Clustering methods such as K-means and Fuzzy C-means do not always arrive at a meaningful segmentation, and often require long computational time. Effective segmentation is required.

For MRI image segmentation, it is important to identify anatomical areas of interest for diagnosis. In this context, we are more concerned with the anatomical region or structure segmentation. We know that the intensity of the MRI image of human tissue is homogeneous and the structure of each tissue is connected, but it is difficult to separate the adjacent tissues due to the small intensity changes and smoothed boundaries between the tissues. The intensity-based segmentation using global thresholding can not segment MRI images properly because of the non-uniform nature of MRI. Edge detection methods such as gradient-based operators, Marr–Hildreth operator, and the improved Canny edge detector [7] are unlikely to provide reliable anatomical region segmentation. Alternatively, edge detection based on image filtering with single scale may over- or under-detect the edges due to the various edge intensities of the different image features, especially when images are corrupted by noise, resulting in incorrect edge detection. Combining the properties of both edge- and region-based segmentation methods, this paper considers the homogeneous region detection in the edge map derived from multi-resolution edge detection, after which an automatic thresholding is employed to eliminate the over-selected regions.

Knowing that the purpose of edge detection is to generate an edge map based on the distribution of the intensity discontinuity of the image, we can define the region to be

* Corresponding author. Tel.: +1-212-305-3566; fax: +1-212-305-1864.
E-mail address: ht145@columbia.edu (H. Tang).

0895-6111/00/$ - see front matter
PII: S0895-6111(00)00037-9

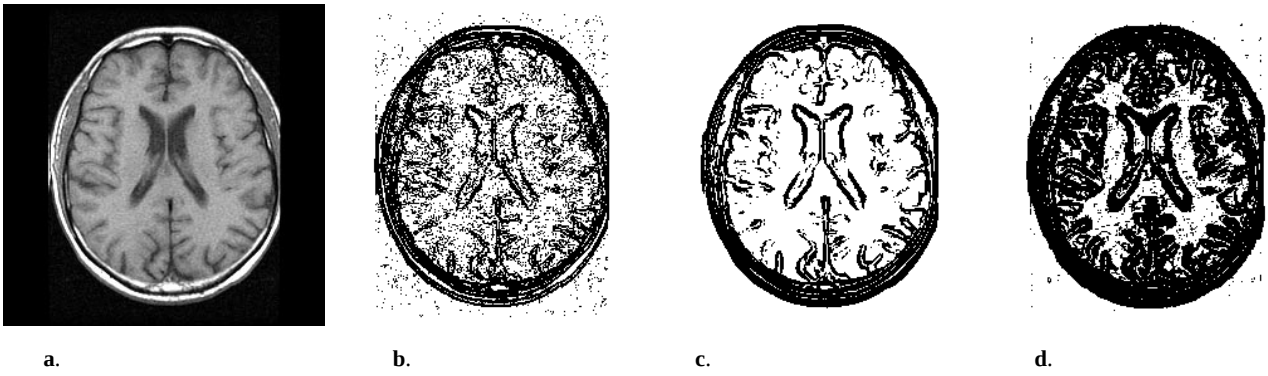

a. **b**. **c**. **d**.

Fig. 1. Edge maps edge detector (Canny Operator) of different scale. (a) Original MRI T1 image. (b) Edge map at $\sigma = 0.5$. (c) Edge map at $\sigma = 2$ with higher threshold. (d) Edge map at $\sigma = 2$ with lower threshold.

homogeneous if the edginess measure is small enough. For MRI brain images, the gray level discontinuity is small between white and gray matter. Therefore, highly sensitive edge detection is required to discriminate between white and gray matter. The edge map derived from the edge detector of different scales represents the edges of different strengths and accuracy. The smaller the scale, the finer and more accurate the edges. However, the edge detector of a small scale is also sensitive to noise. Here, we employed the Canny operator [7] (the first derivative of Gaussian) as our edge detector because of its good localization and high S/N output properties. It is used in the discontinuity measurement of an image in this paper.

Considering the multi-scale nature of the edges and structures in an image, a multi-scale edge detector is used to represent significant edges on the outer and inner surfaces of the brain and detailed edges inside the brain. Fig. 1a shows the original T1 weighted image, Fig. 1b shows the edge map of the small scale $\sigma = 0.5$, which represents finer edge components. Fig. 1c shows the edge map of the larger scale $\sigma = 2$, which represents coarser edge points. Fig. 1d shows the edge map of the scale $\sigma = 2$ with the smaller threshold to select edge points, which represents the finer structures of the homogeneous regions. From Fig. 1, we can see that the edge detector of smaller scale yields finer and accurate edge points, but at the same time selects the noise as edges. The edge detector of the larger scale detects significant edges, thus suppresses noise, but loses detailed edges and accuracy. On the other hand, when decreasing the threshold during the edge selection, discontinuous and homogeneous regions are separated. The smaller the threshold, the finer the structure of the homogeneous regions, but noise may be selected in the homogeneous regions. For images having different structures to be segmented, especially when the images are corrupted with noise, such as MRI images, it is difficult to determine the scale and threshold factors of the edge detector. Thus, multi-resolution edge detection using multi-scale filtering has been considered for the MRI brain tissue segmentation.

Here we referenced the multi-resolution edge detection technique proposed in Ref. [8], detecting both edges and homogeneous regions in different resolution images acquired using multi-scale edge filtering. The application of MRI white matter segmentation is presented here as an example, illustrating how the image is separated into discontinuous regions (edges) and homogeneous regions in different resolutions. The homogeneous region belonging to a connected area can be selected using region-growing method.

Additionally, if the homogeneous region contains many different contents having only small intensity variance, an automatic threshold selection method is used to do the modified region segmentation in the homogeneous ROI image. Finally, in MRI brain image segmentation, both T1 and T2 images are used in effectively and quickly segmenting the different brain tissues in images. Due to the connectivity of the brain tissue in MRI image, region subtraction method is used to acquire a particular brain tissue image according to the resulted white matter image.

2. A multi-resolution edge detection method

The purpose of multi-resolution image analysis is to decompose the image into multi-frequency representations to visualize contents of interest in variable resolutions. Multi-scale filtering such as the Canny operator and the Monga–Deriche filter [9] can detect the edges in the low contrast or low S/N images. They are good edge detectors because they follow the optimal filter design criteria: good localization and high S/N output. By adjusting the scale from low to high, edges from fine to coarse can be obtained. We here employed a multi-resolution edge detection concept [8] to segment both edges and structures. Instead of using the local statistic standard deviation as the edginess measure, we defined a $T_{i,j}$ as the discontinuity measurement using the Canny edge detector:

$$T_{i,j} = G'_{\sigma_n}(f_{i,j}), \tag{1}$$

where $f_{i,j}$ is the original image with the size of $W \times H$, $i \in$

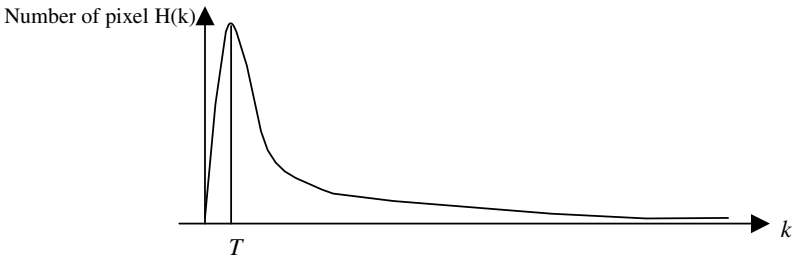

Fig. 2. The distribution of discontinuity measurement.

$[0, W-1]$, $j \in [1, H-1]$, $\sigma_n (n = 1, \ldots, N)$ the scale of the edge detector in the nth decomposition step, $G'_{\sigma_n}(f_{i,j})$ the first derivative of Gaussian function, representing the Canny operator. A pixel belongs to a homogeneous region or an edge region if its discontinuity measurement is less or larger than a proper threshold. The threshold can be automatically derived using the method in Ref. [8]. Suppose $H(k)$ *is* the histogram of $T_{i,j}$, and T is the maximum peak location of the histogram of the discontinuity measurement:

$$H(T) = \mathrm{Max}[H(k)], \quad (k = 1, \ldots, \mathrm{Max}(T_{i,j})). \tag{2}$$

Hence, T can be used as the threshold to separate the image into two images: candidate edge map image $e_{i,j}$ and homogeneous region map image $h_{i,j}$. Fig. 2 shows the example of the discontinuity measurement distribution. Here, the region having the $T_{i,j}$ smaller than T is determined as the homogeneous region at the corresponding resolution.

At the onset of the multi-resolution image decomposition, a small scale σ_0 is used to derive an edge candidate map with sufficient pixels for use in the further multi-resolution decomposition of the image. Using smaller σ_0 is to select any possible candidate edge points, $e^0_{i,j} = 0$, with higher resolution and accuracy. We then begin the multi-resolution decomposition based on the candidate edge points. Knowing that the discontinuity measurement at the noise point is relatively small in low resolution, to suppress the noise in the homogeneous region, we begin with the edge detector of the largest scale (lowest resolution) to get a discontinuity measurement distribution only at the location of the candidate edge points. We then use the threshold derived from the peak location of the discontinuity distribution to remove the larger intensity change points in the homogeneous region. The following decomposition steps recursively separate the regions with a decreasing scale, which means an increasing resolution. The final edge map represents the edges of the finest resolution and strongest discontinuity, and the homogeneous region map in the lowest resolution (largest scale) represents the most homogeneous area in an image.

In our application, the small scale σ_0 is set to $0.5 \sim 1$, the scales in multi-resolution decomposition are set to $0.3 \sim 2.0$, and the scale increment is set to $0.2 \sim 1$. Proper scales should be selected to make sure that the edge detection is not blurred at each resolution. Alternatively, the edge detection can also differentiate the spatial properties among adjacent regions at different resolutions using the multiple scales. Given the proper scale σ_0, and decreasing $\sigma_n (n = 1, 2, \ldots, \sigma_n > \sigma_0)$ after each decomposition to separate finer details in each resolution, we can get a group of multi-resolution image representation. The multi-resolution decomposition procedure is as follows:

1. $n = 0$, $e^0_{i,j} = 0$, $i \in (0, W)$, $j \in (0, H)$, gives a small σ_0.
2. Compute threshold T from $T_{i,j}$ at pixel (i,j) where $e^n_{i,j} = 0$.
3. With threshold T, we can get two binary images, $h^n_{i,j}$ and $e^n_{i,j}$: $h^n_{i,j} = 0$, $e^n_{i,j} = 1$ if $T_{i,j} <= T$; $e^n_{i,j} = 0$ if $T_{ij} > T$.
4. $n = n + 1$, given scale σ_n (decreases with n increase), then go to 2.
5. Repeat 2–4. We can get n groups of multi-resolution image representation.

In multi-resolution brain image representation, we are more interested in localizing different structures in the brain. White matter region is recognized first in the multi-resolution edge maps.

As an example, we applied the above multi-resolution representation and segmentation procedure to a T2-weighted MRI brain image from Visible Human shown in Fig. 3a and b shows the initial candidate edge map at $n = 0$ and $\sigma_0 = 1$, from which multi-resolution image edge maps and homogeneous region maps Fig. 3c–j was derived.

2.1. A simple brain tissue segmentation using region-based image segmentation and subtraction

In multi-resolution decomposition, we find that the nth edge map $e^n_{i,j} = 0$ is separated into the next finer edge map $e^{n+1}_{i,j} = 0$ and the homogeneous map $h^{n+1}_{i,j} = 0$ whose components belong to a less homogeneous region. In the edge detection of MRI brain images, the significant edges can be detected around the boundaries of the brain surfaces and the adjacent place of the white and gray matter. From the multi-resolution edge map images shown in Fig. 3, we can see that the edges become finer and more accurate where the abrupt intensity change occurs and the homogeneous regions inside the brain become larger. In the homogeneous map images, we can see that the homogeneous region becomes courser when the scale of the edge detector becomes smaller. With the edge map information, we can separate the structure of the homogeneous region by simply using the region-growing method.

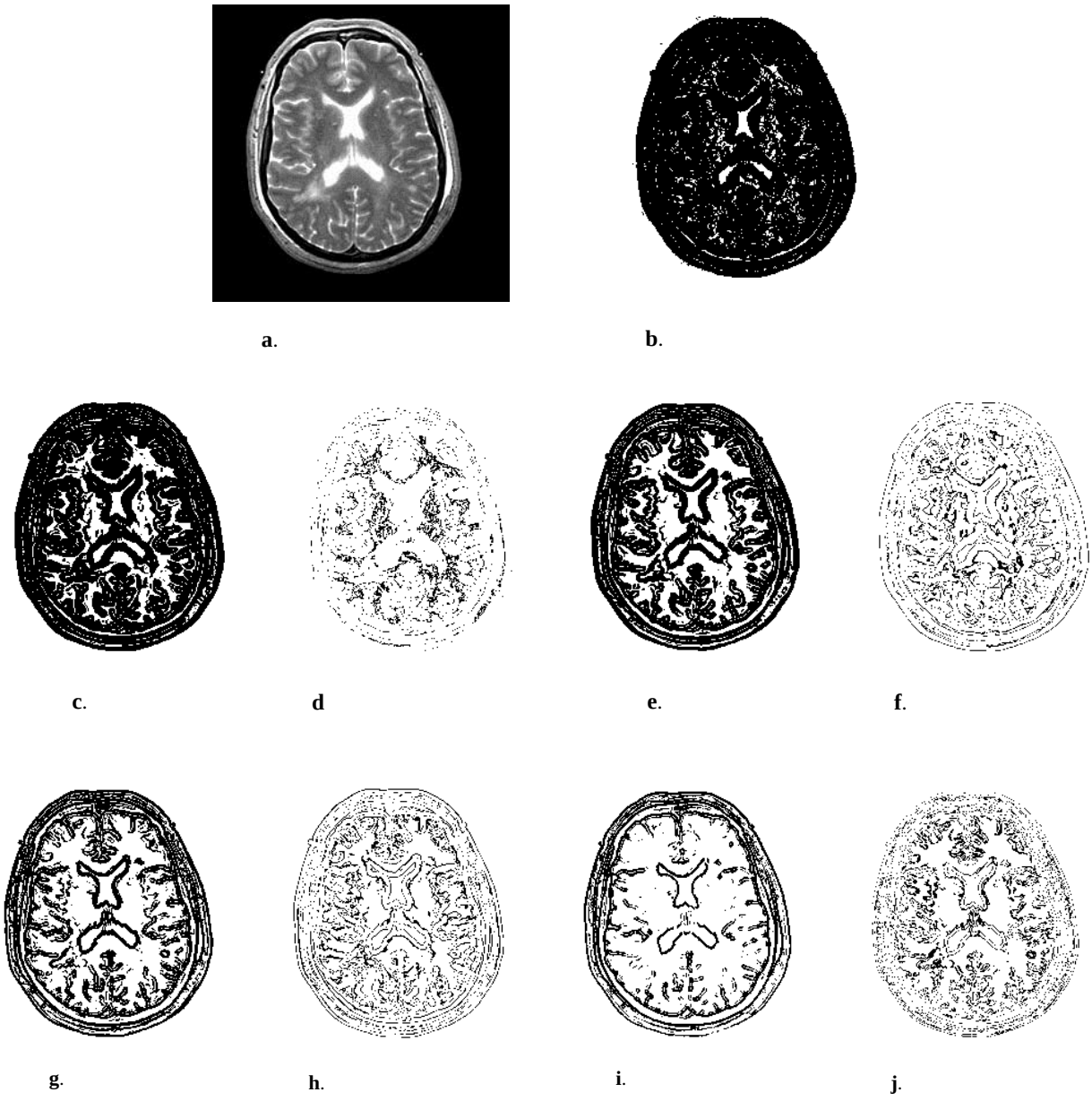

Fig. 3. Multi-resolution segmentation and representation of a T2 weighted MRI brain image from Visible Human. (a) Original MRI T2 image. (b) Initial candidate edge map ($n = 0$, $e_{ij}^0 = 0$, scale $\sigma_0 = 1$). (c) Edge map ($n = 1$, $e_{ij}^1 = 0$, $\sigma_1 = 1.5$). (d) Homogeneous Region map with $h_{ij}^1 = 0$. (e) Edge map ($n = 2$, $e_{ij}^2 = 0$, $\sigma_2 = 1$). (f) Homogeneous Region map with $h_{ij}^2 = 0$. (g) Edge map ($n = 3$, $e_{ij}^3 = 0$, $\sigma_3 = 0.5$). (h) Homogeneous Region map with $h_{ij}^3 = 0$. (i) Finest edge map ($n = 4$, $e_{ij}^4 = 0$, $\sigma_4 = 0.3$). (j) Homogeneous Region map with $h_{ij}^4 = 0$.

2.1.1. Homogeneous structure region segmentation and subtraction

Using the tissue connectivity, we then applied a region-based procedure to segment structures of interest in the brain. Based on the delineation of white matter structure and CSF in Figs. 3e and 4a was derived using region growing in the white matter structure. The middle region of the brain in Fig. 3i contains most of the white and gray matter, in which we applied the subtractions. Results are shown in Fig. 4b–d, illustrating gray matter and CSF.

Although we derived the preliminary segmentation results shown in Fig. 4, this does not imply that the region subtraction method is always reproducible. The MRI images are corrupted always by noise, and the intensity difference is hard to see between white and gray matter. Therefore, in the following section, we will discuss the method to modify the segmentation of ROI image derived from the region-growing in homogeneous regions.

2.1.2. Homogeneous structure region segmentation in different scale

The homogeneous regions seen in the edge maps

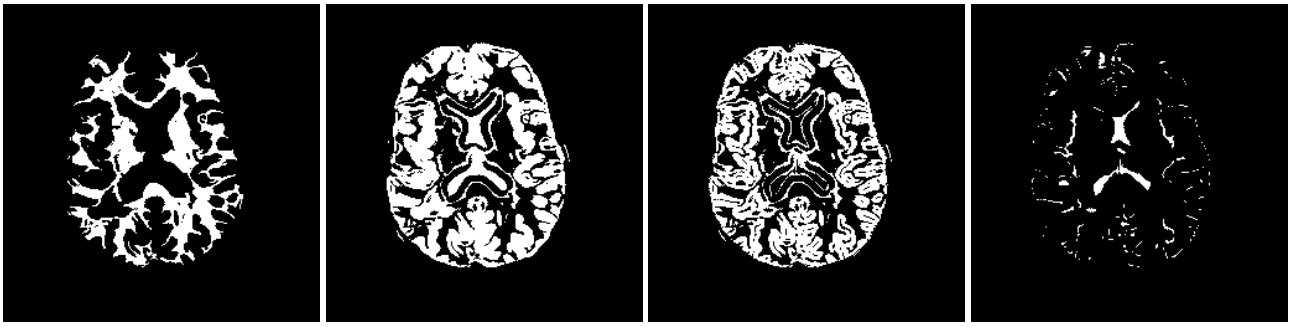

a. **b**. **c**. **d**.

Fig. 4. Segmentation of a T2 weighted brain image using region-based methods (region-growing and region subtraction). (a) Region-growing in Fig. 3e. (b) Subtract a from Fig. 3i. (c) Subtract Fig. 3e from b. (d) Subtract c from b.

$e^n_{i,j} = 0$ of different resolutions showed the multi-scale nature of brain structures. Fig. 5 shows the multi-resolution homogeneous structure representation of the T1 weighted MRI image shown in Fig. 1a, in which the brain tissue contains a white matter region, a gray matter region, and the CSF. The gray and white matter regions can be selected as a single region when the image is represented at the scale that allows for large intensity variation. To separate the white matter region, we should use the edge detector with a smaller scale that is sensitive to small intensity variations. Given $\sigma_0 = 1$, Fig. 5a shows the segmentation of the homogeneous region in the first decomposition with the scale $\sigma_1 = 1.5$. The noises in the homogeneous region are eliminated after this largest scale decomposition. Fig. 5b shows the segmentation of the region in the second decomposition with $\sigma_2 = 1$, where more homogeneous regions are derived. Fig. 5c shows the segmentation of the region in the third decomposition with $\sigma_3 = 0.5$.

2.2. Threshold selection criterion and the modified region segmentation method

In real applications using the region-growing method to segment the homogeneous regions, we encountered the problem of under- or over-selection of brain white matter. When images are corrupt with noise, and the intensity differences among white, gray, and some of the CSF matters are small, these different tissues may be segmented into the same homogeneous regions using the multi-resolution edge detection and region segmentation procedure. Here, a modified region segmentation method based on an automatic threshold selection algorithm is presented to separate the white matter more accurately in the ROI image derived from the homogeneous region segmentation of the multi-resolution edge map images.

Fig. 6a is a T2 weighted MRI brain image. Fig. 6b represents the preliminary white matter structures, which are derived from the multi-resolution edge detection and region selection methods. Figs. 5b and 6b show that some of the gray matter and CSF regions are indistinguishable from the white matter region due to the very small intensity variations in these regions. They are selected in the same homogeneous regions with the white matter using the region-growing method. Knowing that there are small intensity differences

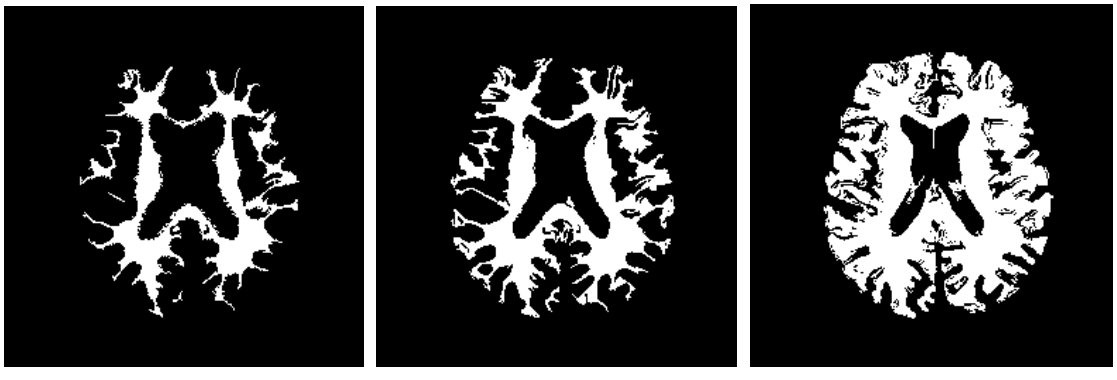

a. **b**. **c**.

Fig. 5. Segmentation of the homogeneous region in T1 weighted brain image shown in Fig. 1a using region-growing method. (a) Region-growing in homogenous region in the first decomposition ($\sigma_1 = 1.5$). (b) Region-growing in homogenous region in the second decomposition ($\sigma_2 = 1$). (c) Region-growing in homogenous region in the third decomposition ($\sigma_3 = 0.5$).

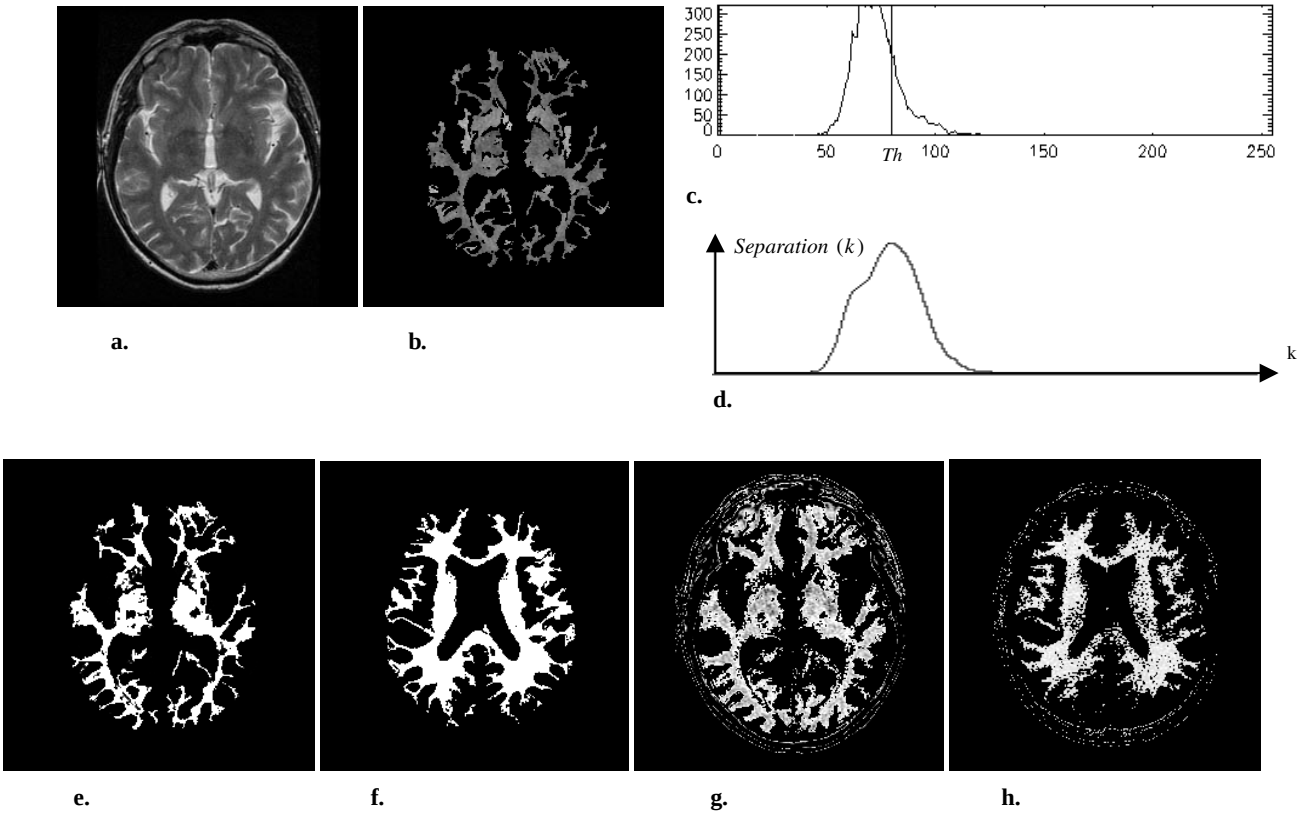

Fig. 6. Modified region segmentation of the white matter in MRI images using an automatic thresholding selection method. (a) Original MRI T2 weighted brain image. (b) Initial white matter region selection (ROI) from a: smooth $(f_{ij}^{a})_{\mathrm{ROI}}$. (c) Intensity distribution(histogram) of the smooth $(f_{ij}^{a})_{\mathrm{ROI}}$ in b. (d) Curve of the seperation function using histogram in c. (e) Modified segmentation of brain white matter in b using threshold *Th* in c. (f) Modified segmentation of brain white matter in Fig. 1a using region selection in Fig. 5b. (g) Segmentation of the white matter in a using thresholding method. (h) Segmentation of the white matter in Fig. 1a using thresholding method.

between different brain tissues, a further segmentation in the homogeneous region containing the over-selected brain tissues is presented using an automatic threshold selection method, leaving only the white matter regions. Since the regions to be eliminated are limited to the small homogeneous regions containing CSF and gray matter, and the large part of the regions belongs to white matter, for example Fig. 6b, the following automatic thresholding method is used to separate the white matter regions from the initial homogeneous region image.

2.2.1. Automatic threshold selection

At first, we use the initial segmented homogeneous region as a mask, which is defined as the ROI. The pixels of the original image that are located in the ROI: $(f_{i,j})_{\mathrm{ROI}}$ were selected, as shown in Fig. 6b. To select a threshold for separating the different contents that have small intensity variations, we modified the Otsu's threshold selection method [10] by defining a different separation measurement function to evaluate the "goodness" of the threshold and then select an optimal threshold. Suppose there are N gray levels in the ROI of the image: I_{ROI}, which is from $I_{\min}$ to $I_{\max}$, the gray level distribution of the image of ROI, the histogram is:

$$\mathrm{Histogram}(i) = n_i, \quad i \in [I_{\min}, I_{\max}], \quad I_{\min} = \mathrm{MIN}(I_{\mathrm{ROI}}),$$
$$I_{\max} = \mathrm{MAX}(I_{\mathrm{ROI}}), \tag{3}$$

where n_i is the number of pixels at gray level i. To separate the pixels into two classes, given that the first class contains the gray levels: $I_{\min} \le I_1 \le k$, and the second class contains the gray levels: $k < I_2 \le I_{\max}$, the mean level of each class should be:

$$\mathrm{mean}_1(k) = \sum_{i=I_{\min}}^{k} \mathrm{Histogram}(i)/N_1, \quad N_1 = \sum_{i=I_{\min}}^{k} \mathrm{Histogram}(i), \tag{4}$$

$$\mathrm{mean}_2(k) = \sum_{i=k+1}^{I_{\max}} \mathrm{Histogram}(i)/N_2,$$
$$N_2 = \sum_{i=k+1}^{I_{\max}} \mathrm{Histogram}(i) \tag{5}$$

The mean level of the ROI is given by

$$\text{mean}_{\text{ROI}} = \sum_{i=I_{\min}}^{I_{\max}} \text{Histogram}(i)/N, \quad N = \sum_{i=I_{\min}}^{I_{\max}} \text{Histogram}(i) \tag{6}$$

Thus, the probability of each class in the ROI should be

$$P_1(k) = N_1/N, \quad P_2(k) = N_2/N \tag{7}$$

To know if k is the better threshold to separate the two classes, a criterion is introduced and named as the separation measurement function by the following equation:

$$\text{Separation}(k) = P_1(k) \times P_2(k) \times [(\text{mean}_1(k) - \text{mean}_{\text{ROI}})^2 + \text{mean}_2(k) - \text{mean}_{\text{ROI}})^2], \tag{8}$$

where $k = I_{\min}, \ldots, I_{\max}$.

In the above separation measurement function, if k is the best separation threshold, Separation(k) will be at its maximum value. Thus, the threshold selection is an automatic procedure, which searches for a threshold k that maximizes the above function. The optimal $k_{\text{threshold}}$ is located at:

$$\text{Separation}(k_{\text{threshold}}) = \max_{I_{\min} \le k \le I_{\max}} (\text{Separation}(k)). \tag{9}$$

In an MRI image, the intensity distribution of most pixels in an ROI should be in a particular range R_{ROI}. For the pixels such as noise, whose histogram is not distributed in the range R_{ROI}, after being separated as a class at threshold k, the class probability is always small, resulting in a quite small Separation(k). Using the above threshold selection criteria, the noise pixels can thus avoid selection as a class at the threshold k, and the optimal threshold $k_{\text{threshold}}$ can be located inside the range R_{ROI}.

2.2.2. Modified region segmentation in noisy image

If the image has been corrupted with noise, the above method may result in an incorrect threshold selection or unsmoothed region segmentation. Instead of using the original image $f_{i,j}$ in ROI, we use the smoothed image Smooth($f_{i,j}$) in ROI: Smooth($f_{i,j}$)$_{\text{ROI}}$ to derive the corresponding gray level distribution:

$$\text{Histogram}(i) = ni, \quad i \in [I_{\min}, I_{\max}], \text{ where } I_{\min} = \text{MIN}(\text{Smooth}(f_{ij})_{\text{ROI}}), \quad I_{\max} = \text{MAX}(\text{Smooth}(f_{i,j})_{\text{ROI}}). \tag{10}$$

The smoothed image is derived using a low-pass filtering method such as Gaussian operator. On identifying the optimal threshold k, $I_{\min} \le k \le I_{\max}$, regions are separated in the smoothed image. The segmented region may have better connectivity and intensity homogeneity. For the MRI brain image segmentation, image smoothing should be employed before selecting the image in ROI.

In Fig. 6b, instead of using ($f_{i,j}$)$_{\text{ROI}}$, Smooth($f_{i,j}$)$_{\text{ROI}}$ is used as the initial image of ROI. Fig. 6c shows the histogram of the gray levels in the ROI image in Fig. 6b. *Th* in Fig. 6c is the corresponding threshold used to separate white matter from the image in Fig. 6b, which is derived from the maximum location of the separation measurement Separation(k) shown in Fig. 6d. The white matter segmentation of Fig. 6a is shown in Fig. 6e and f shows the modified segmentation of white matter in Fig. 1a using the initial region selection shown in Fig. 5b, representing the more reasonable white matter structures. Compared to the thresholding segmentation method used to directly separate the white matter from the original image, the modified region segmentation method based on the above threshold selection criteria results in cleaner and finer brain tissue structures. For example, the white matter segmentation in Figs. 1a and 6a based on conventional gray level thresholding are shown in Fig. 6g and h. The results are not ideal because of the non-uniform nature of the MRI image and the gray level overlap among different tissues.

2.3. Segmentation of the brain tissue using both T1 and T2 images

We presented the brain tissue segmentation based on a multi-resolution edge detection method and modified region segmentation method. We also mentioned the segmentation based on region subtraction between region images acquired during multi-resolution edge detection procedure. It is easier to segment CSF matter using conventional segmentation such as the gray level thresholding method. However, where both T1 and T2 images of the same section are available, both can be used in brain image segmentation.

Example on multiple brain tissue segmentation using T1 and T2 images of the same section is illustrated in Fig. 7. It is shown that CSF matter has a higher gray level in T2 images, while it has a lower gray level in T1 images. We simply apply image subtraction to get the following images. Fig. 7a shows the T2 weighted MRI brain image scanned at the same location as the T1 image shown in Fig. 1a. The CSF matter is expressed when subtracting the T1 image in Fig. 1a from the T2 image in Fig. 7a, the result is shown in Fig. 7b and c shows the inner surface of the brain obtained by subtracting the T2 image from the negative T1 image.

From the result in Fig. 7c, we can select the region inside the inner surface of the brain using the region-growing method and acquire a mask shown in Fig. 8a and b shows the image inside the brain region from Fig. 7a. Knowing the distribution of the CSF and the white matter, we can get the resulting gray matter distribution by subtracting the segmented CSF and white matter images from the original image, the gray matter segmentation is shown in Fig. 8c. If we use the modified region segmentation method to re-segment the regions shown in Fig. 5d, which contains white matter, gray matter and some of the CSF matter, we can get a modified region segmentation that consists mainly of white and gray matter. After applying the subtraction of the

a. b. c.

Fig. 7. Image subtraction between T1 and T2 weighted MRI images scanned at the same location. (a) Original T2 weighted MRI brain image scanned at the same location as the T1 image shown in Fig. 1a. (b) subtraction between a and Fig. 1a, illustrating most of the CSF matter. (c) subtraction between negative T1 image in Fig. 1a and T2 image in a.

corresponding white matter region shown in Fig. 6f derived from the modified region segmentation, we can get the resulting gray matter structure shown in Fig. 8d, which is similar to the gray matter segmentation shown in Fig. 8c.

2.4. 3D MRI brain image segmentation and visualization

Using the segmentation methods proposed in this paper, 2D segmentation results of MRI brain images have been presented. The methods can be extended to 3D images, in which the images can be segmented slice by slice or directly in 3D. In the direct 3D cases, the multi-scale image edge detection can be realized using a 3D Monga–Deriche filtering method [9], and the region selection can be realized using 3D region-growing method. Fig. 9 gives 3D results using the extended direct 3D-segmentation method. Fig. 9a shows the front view of the volume rendering of the human white matter, Fig. 9b shows the volume rendering of the white matter seen from section S1 shown in Fig. 9a and c shows the volume rendering of the white matter seen from the top of the brain.

3. Discussion

The proposed MRI brain image segmentation method based on multi-resolution edge detection, region selection, and automatic intensity thresholding methods has the potential advantage of directly and simultaneously illustrating brain tissue structures in MRI images, in which those structures are not easily distinguished due to the small intensity variation. Since the scale of the low-pass filter is adjustable, the multi-resolution representation can be made more adaptable and meaningful. Both 2D and 3D MRI brain image segmentation results show that the method is effective and robust, even though the images are corrupted with noises. Such image segmentation can also yield isolated brain structures such as white matter, gray matter and CSF. Compared with the conventional thresholding method, the proposed segmentation method reduces noise in homogeneous region while preserving fine structures of the brain tissues. Therefore, it can be used in conjunction with other algorithms, such as template matching, for accurate brain tissue classification, in which case our segmentation results can be used as templates and elastically matched to real brain tissues.

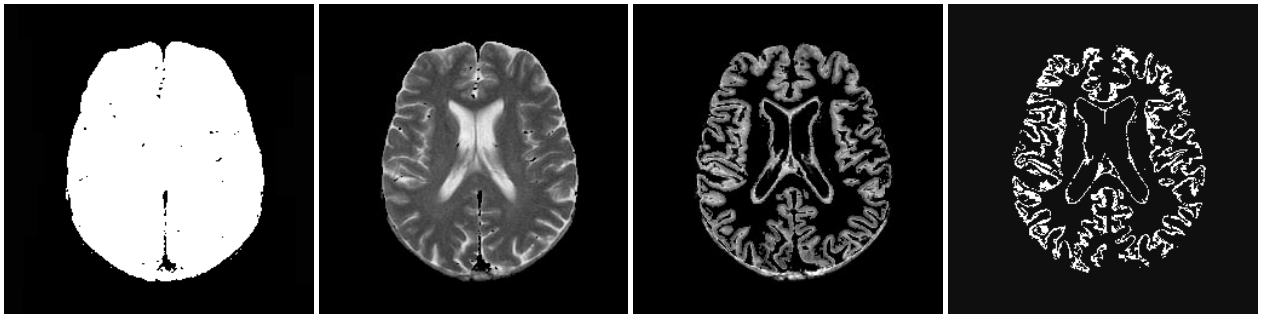

a. b. c. d.

Fig. 8. Image subtraction used in gray matter segmentation. (a) Mask of the brain region in Fig. 7a. (b) Image inside the brain region in using the mask in a. (c) Gray matter in Fig. 7a obtained by subtracting Fig. 6f from b. (d) Gray matter region in Fig. 7a obtained by subtracting Fig. 6f from the re-segmentation of Fig. 5c.

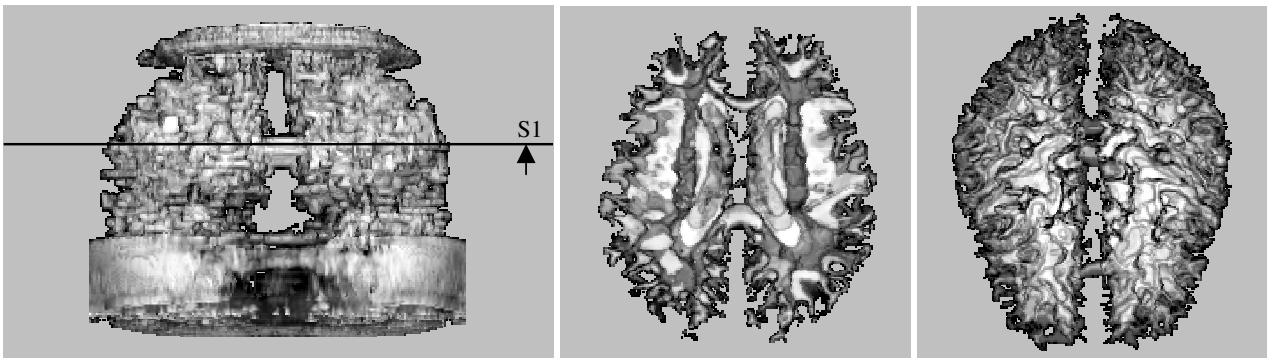

Fig. 9. 3D Visualization of the white matter inside human brain. (a) Front view of volume rendering of the white matter. (b) Visualize the white matter from section S1. (c) Visualize the white matter from top.

4. Summary

An MRI brain image segmentation method based on multi-resolution edge detection, region selection, and automatic intensity thresholding methods is presented. The multi-resolution MRI brain image representation and brain tissue segmentation results are given. This segmentation method integrated both image regional and intensity information, combined image filtering, region-growing, and automatic intensity thresholding methods, can segment the white matter, gray matter and CSF in an MRI brain image. The multi-resolution edge detection is based on the multi-scale image filtering method. The automatic intensity thresholding method is based on a modified threshold selection method presented in this paper. Because white matter is located in the homogeneous region, it can be separated using region growing due to the connectivity of the brain tissue. Using the region subtraction, we can separate other brain tissues. Finally, brain image segmentation using both T1 and T2 weighted images is described. The presented method can be used to segment both T1 and T2 weighted MRI brain images, and can be extended to 3D data sets, examples of the 3D white matter visualization are presented.

The performance of the brain image segmentation is shown by the comparison with the conventional thresholding method. It is obvious that the proposed method reduces noise in homogeneous region while preserving fine structures of the brain tissues. The proposed method can be combined with other image segmentation and pattern recognition techniques with a proper edginess measure and region selection in various resolutions, to increase the accuracy of the localization and quantification of brain tissues.

References

[1] Clarke LP, Velthuizen RP, Camacho MA, Heine JJ. Segmentation: methods and applications. Magnetic Resonance Imaging 1995;13(3):343–68.
[2] Suckling J, Sigmundsson T, Greenwood K, Bullmore ET. Modified fuzzy clustering algorithm for operator independent brain tissue classification of dual echo MR images. Magnetic Resonance Imaging 1999;17(7):1065–76.
[3] Mark T, Narendra A. Multiscale image segmentation by integrated edge and region detection. IEEE Transactions on Image Processing 1997;6(5):642–55.
[4] Mark B. Skouson, Zhi-Pei Liang. Template deformation by maximizing mutual information. Proceeding of the 1st Joint Meeting of BMES & EMBS, Atlanta, 1999. p. 1162.
[5] Gary CE. Deformable templates using large deformation kenematics. IEEE Transactions on Image Processing 1996;5(10):1435–47.
[6] Chen C, Luo J, Parker KJ. Image segmentation via adaptive K-mean clustering and knowledge-based morphological operations with biomedical applications. IEEE Transactions on Image Processing 1998;7(12):1673–83.
[7] Canny J. Computational approach to edge detection. IEEE Transactions on PAMI 1986;8(6):679–98.
[8] Deok JP, Kwon NM, Rae-Hong P. Multiresolution edge detection techniques. Pattern Recognition 1995;28(2):211–29.
[9] Monga O, Rachid D. 3D edge detection using recursive filter: application to scanner images. CVGIP: Image Understanding 1991;53(1):76–87.
[10] Nobuyuki O. A threshold selection method from gray-level histograms. IEEE Transactions on SMC 1979;9(1):62–6.